Functional Analysis of Basic Transcription Element Binding Protein by Gene Targeting Technology

Masanobu Morita,[1]† Akira Kobayashi,[1]‡ Toshiharu Yamashita,[1]‡ Tomomasa Shimanuki,[1]
Osamu Nakajima,[2] Satoru Takahashi,[2] Shiro Ikegami,[3] Kaoru Inokuchi,[3]
Keisuke Yamashita,[4] Masayuki Yamamoto,[2]
and Yoshiaki Fujii-Kuriyama[1,5]*

*Department of Biomolecular Science, Graduate School of Life Science, Tohoku University, Sendai 980-8578,[1] Center
for Tsukuba Advanced Research Alliance and Institute for Basic Medical Sciences, University of Tsukuba,
Tsukuba 305-8577,[2] Mitsubishi Kagaku Institute of Life Sciences, Machida, Tokyo 194-8511,[3]
Department of Anatomy and Developmental Biology, Graduate School of Biomedical
Sciences, Hiroshima University, Hiroshima 734-8551,[4] and Core Research for Evolutionary
Science and Technology, Japan Science and Technology, Tokyo,[5] Japan*

Received 14 June 2002/Returned for modification 7 October 2002/Accepted 19 December 2002

Basic transcription element binding protein (BTEB) is a transcription factor with a characteristic zinc finger motif and is most remarkably enhanced by thyroid hormone T_3 treatment (R. J. Denver et al., J. Biol. Chem. 272:8179-8188, 1997). To investigate the function of BTEB per se and to touch on the effects of T_3 (3,5,3′-triiodothyronine) on mouse development, we generated BTEB-deficient mice by gene knockout technology. Homologous $BTEB^{-/-}$ mutant mice were bred according to apparently normal Mendelian genetics, matured normally, and were fertile. Mutant mice could survive for at least 2 years without evident pathological defects. From the expression of *lacZ*, which was inserted into the reading frame of the BTEB gene, BTEB showed a characteristic tissue-specific expression profile during the developmental process of brain and bone. Dramatically increased expression of BTEB was observed in Purkinje cells of the cerebellum and pyramidal cell layers of the hippocampus at P7 when synapses start to form in the brain. Although general behavioral activities such as locomotion, rearing, and speed of movement were not so much affected in the $BTEB^{-/-}$ mutant mice, they showed clearly reduced activity levels in rotorod and contextual fear-conditioning tests; this finding was probably due to defective functions of the cerebellum, hippocampus, and amygdala.

The basic transcription element binding protein (BTEB) is a transcription factor with a triple-repeat zinc finger motif and was originally isolated as a protein that binds to the basic transcription element in the CYP1A1 gene promoter, a GC-box sequence identified by South-Western screening (15). This protein has a high sequence similarity to the Sp1 family of transcription factors, primarily in the zinc finger region (DNA-binding domain). It has been demonstrated that BTEB and Sp1 recognize and bind the same GC-box sequence with almost identical affinity (29). Beyond the DNA-binding domain, however, the two proteins share little sequence similarity. Interestingly, although BTEB mRNA is ubiquitously expressed in various tissues such as the brain, testis, kidney, and liver, the mRNA appears to be translated only in the brain (14). In the same vein, the BTEB mRNA that is expressed in HeLa and Neuro-2A cells has been reported to be translated only in

Neuro-2A cells (14). These results show that expression of the BTEB gene is regulated posttranscriptionally in a tissue- and cell-specific manner.

It is known that thyroid hormone T_3 (3,5,3′-triiodothyronine) is essential for normal development of the vertebrate central nervous system (CNS) (18, 26, 34). Defective levels of thyroid hormone cause abnormal development of the vertebrate CNS, resulting in neurological defects, including irreversible mental retardation (18, 26). The effects of T_3 are known to be mediated by the cognate thyroid hormone receptors, which heterodimerize with retinoid X receptor (20, 33) before binding to the TRE sequence in the promoter of target genes. However, relatively little is known about the functional role of T_3 in brain development because the information regarding the target genes is limited. Differential hybridization was performed to search for T_3-regulated genes in vertebrates such as the frog and the rat (3, 4, 5, 10, 11, 24, 32, 35), and the BTEB gene was identified as one of the most distinct T_3-responsive genes in the *Xenopus* tadpole (3, 4). The enhanced expression of the BTEB gene in response to T_3 has also been confirmed in the developing CNS of the rodent and was demonstrated to be a transcriptional event by a nuclear run-on assay (4). Overexpression of the BTEB gene in the cultured neuroblastoma cell line Neuro-2A stimulated neurite outgrowth of the cells but did not induce acetylcholine esterase activity, indicating that BTEB fulfilled at least a partial role in the multiple T_3 actions in vertebrate neurogenesis (4).

* Corresponding author. Mailing address: TARA Center, University of Tsukuba, Tennoudai 1-1-1, Tsukuba, Ibaraki 305-8577, Japan. Phone: 81-298-53-7323. Fax: 81-298-53-7318. E-mail: ykfujii@tara.tskuba.ac.jp.
† Present address: The Salk Institute for Biological Studies, La Jolla, CA 92037-1099.
‡ Present address: Center for Tsukuba Advanced Research Alliance and Institute for Basic Medical Sciences, University of Tsukuba, Tsukuba, Ibaraki 305-8577, Japan.
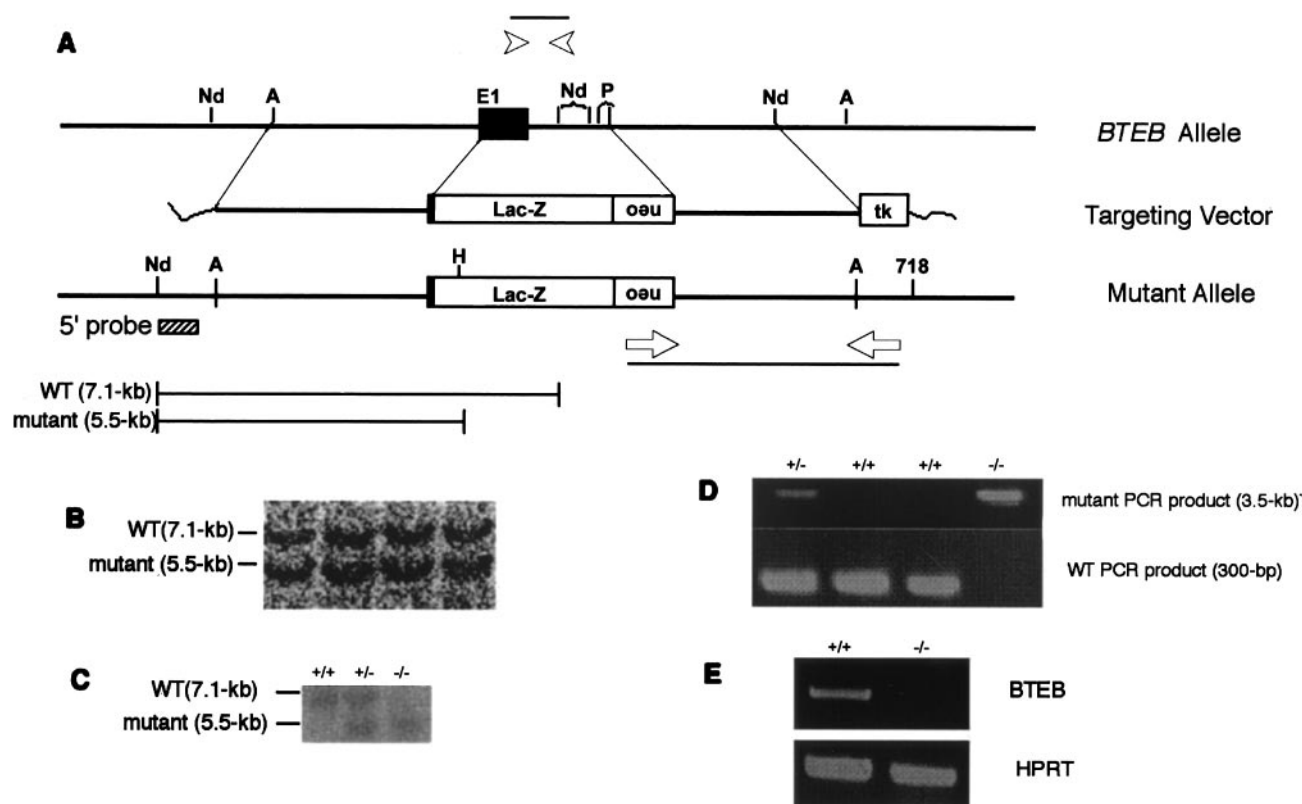
FIG. 1. Mutation of mouse *BTEB* gene. (A) Outline of targeting vector and restriction maps around the first exon. Arrowheads indicate the sites of primers used to distinguish the wild-type BTEB gene from that of the mutant. neo indicates the neomycin-resistant gene, and tk is the thymidine kinase gene under the control of the herpes simplex virus promoter. The sizes of the DNA fragments digested with *Nde*I are shown below. (B and C) DNA blot analysis of DNA from recombinant cells and mouse tails, respectively. Genomic DNAs were prepared from ES cells and mouse tail, digested with *Nde*I and *Hin*dIII, and electrophoresed in 1% agarose, followed by hybridization with the 5′ probe indicated in panel A. (D) Genotyping of the BTEB locus from offspring. PCR analyses were carried out with genomic DNAs from offspring generated by cross-mating heterozygous BTEB$^{+/-}$ mice. The primer pairs were used as described in panel A, and the PCR products were analyzed by agarose gel electrophoresis. (E) RT-PCR analyses of BTEB mRNA expression. RNAs were prepared from the brains of wild-type and mutant mice. RT-PCR of the prepared RNAs was performed with a pair of primers as described in Materials and Methods, and the RT-PCR products were separated by agarose gel electrophoresis. hypoxanthine phosphoribosyltransferase (HPRT) mRNA expression was used as control.

To investigate the functional role of BTEB per se and at least a part of T$_3$ effects on mouse brain development, we generated BTEB gene knockout mice. The *lacZ* gene was inserted into the reading frame of the first exon in BTEB gene by homologous recombination, such that β-galactosidase (β-Gal) expression mimics the expression of BTEB, thereby facilitating the survey of pathological abnormalities due to a lack of BTEB expression.

Homozygous BTEB knockout (BTEB$^{-/-}$) mice were bred by apparently normal Mendelian genetics from a cross between heterozygous BTEB$^{+/-}$ mutant mice and grew normally and were fertile. Expression of BTEB dramatically increased in the brain, especially in the hippocampus and cerebellum, at around postnatal day 7 (P7), the time when synapses begin to mature in the CNS. Examination of general locomotor activities, motor coordination, and memory tasks revealed that BTEB mutant mice exhibit deficits in motor coordination and in learning and memory tasks, which are principally associated with cerebellar and hippocampal functions, respectively.

MATERIALS AND METHODS

Construction of targeting vector. A genomic DNA sequence containing the 5′-flanking region and the first intron of the BTEB gene was isolated from a mouse 129/SV genomic library, with rat BTEB cDNA *Sac*II-*Nsp*V fragment used as a probe. An *Ase*I/*Not*I fragment of 5 kb containing the BTEB promoter and 12 bp of the coding sequence of the first exon was fused in frame with the *lacZ* cassette (*Hin*dIII/*Sma*I fragment of pENL) containing the simian virus 40 T antigen intron and the polyadenylation signal. The 3′ end of the *lacZ* cassette was fused with the *neo* gene cassette (*Xho*I/*Bam*HI fragment of pMC1-neo) in a reverse orientation to the *lacZ* gene for the positive selection, followed by 3.1 kb of a *Pvu*II/*Ase*I fragment of the mouse BTEB gene. This construct was ligated to the thymidine kinase cassette (HSV-TK) at the 3′ end and inserted between the *Eco*RV and *Asp*718 sites of pBluescript for amplification in *Escherichia coli*. The amplified plasmid was linearized by *Kpn*I digestion and used for electroporation.

Targeted disruption of the BTEB gene in ES cells. E14 embryonic stem (ES) cells were cultured, transformed with the targeting vector, and screened by standard methods (9). The linearized targeting vector DNA (80 μg) was electroporated into ES cells (10^7 cells/ml), and the cells were subjected to double selection by using G418 (300 μg/ml) and ganciclovir (2 μM). After 10 days, isolated clones were expanded and genomic DNAs were prepared for determination of homologous recombination.

Blastocysts were harvested from 3.5-day postcoital (dpc) C57BL/6j females and the homologous recombinant ES cells were injected into the blastocoel
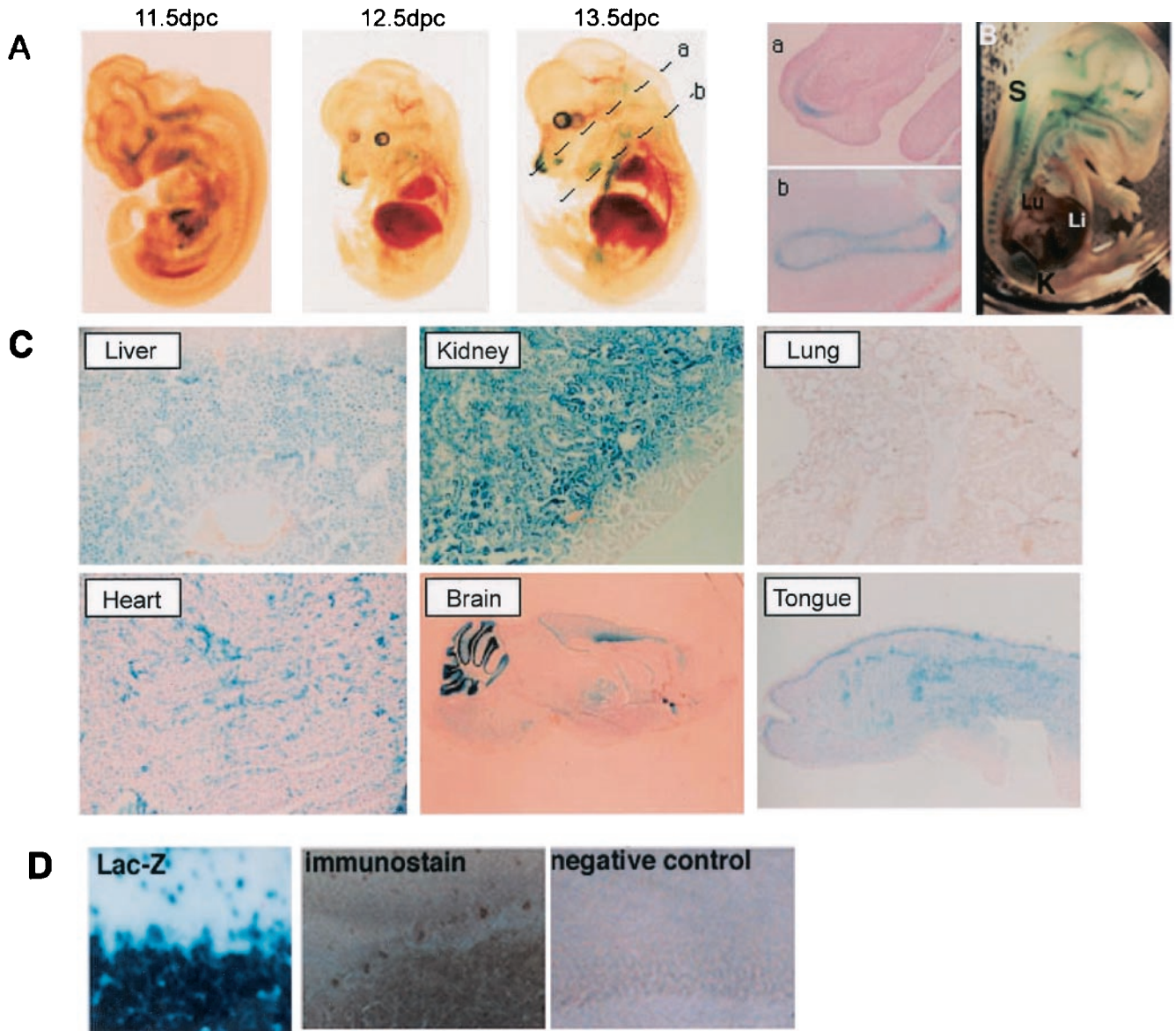
FIG. 2. Expression patterns of BTEB in mouse embryo and adult tissues. (A) Until 11.5 dpc, BTEB was not detected in any organ in mouse embryo. BTEB expression started at 12.5 dpc, and expression was restricted to skeletal tissue. The photos in subpanels a and b are sections indicated by broken lines of BTEB$^{+/-}$ 13.5-dpc embryo with β-Gal staining. Sections a and b show BTEB expression in the cartilage primordium of nasal capsule and the cartilage primordium of rib, respectively. (B) At 15.5 dpc, BTEB expression extended to the spinal cord, kidney, and lung. (C) BTEB expression in adult mouse tissues was detected rather ubiquitously in various tissues, such as liver, kidney, heart, brain, and tongue tissues. Lung tissue was the only tissue for which we could not detect BTEB expression in adult mice and only a weak expression at the embryonic stage. (D) β-Gal expression of the cerebellum in BTEB$^{+/-}$ mice showed almost the same expression pattern as observed with immunostaining with anti-BTEB antibody. A P14 BTEB$^{+/-}$ mouse cerebellum sagittal section was stained with β-Gal, and a BTEB$^{+/+}$ cerebellum sagittal section was analyzed by using immunohistochemistry with anti-BTEB antibody. Both β-Gal staining and immunostaining showed identical positive signals in Purkinje cells and the granular cell layer. The negative control for immunohistochemistry was performed with nonimmune serum (right photo). Abbreviations: S, spinal cord; Lu, lung; K, kidney; Li, liver.

cavities of the 3.5-dpc blastocysts. Injected blastocysts were surgically transferred into uteri of 2.5-dpc pseudopregnant Jcl:ICR mothers (9). Male chimeric pups with an extensive ES cell contribution to their coat color were bred with C57BL/6j females, and germ line transmission of the dominant agouti color marker was assessed in the resulting offspring. Germ line transmission of the defective BTEB allele was screened by the PCR method and subsequently confirmed by DNA blot analysis by using DNA prepared from tails. The primer pair and DNA probe used for the PCR and the DNA blot analysis, respectively, were as follows: the *neo* sequence at the 5′ end, 5′-CAG TCA TAG CCG AAT AGC CTC TCC ACC AAA-3′, and the endogenous BTEB-flanking sequence at

the 3′ end, 5′-CAG TCA TAG CCG AAT AGC CTC TCC ACC AAA-3′ for PCR and the *Nde*I-*Ase*I fragment (1 kb) for DNA blot analysis. PCR analysis consisted of 30 cycles of 98°C for 20 s, 60°C for 45 s, and 68°C for 3 min with LA *Taq* (TaKaRa, Tokyo, Japan). For DNA blot analysis, tail DNAs were digested with *Nde*I and *Hin*dIII and subjected to 1% gel electrophoresis for blot hybridization.

β-Gal staining and TUNEL (terminal deoxynucleotidyltransferase-mediated dUTP-biotin nick end labeling). β-Gal staining was carried out as described previously (9), with embryos or adult tissues fixed in phosphate-buffered saline (PBS) containing 2% paraformaldehyde, 0.2% glutaraldehyde, and 0.05% Non-
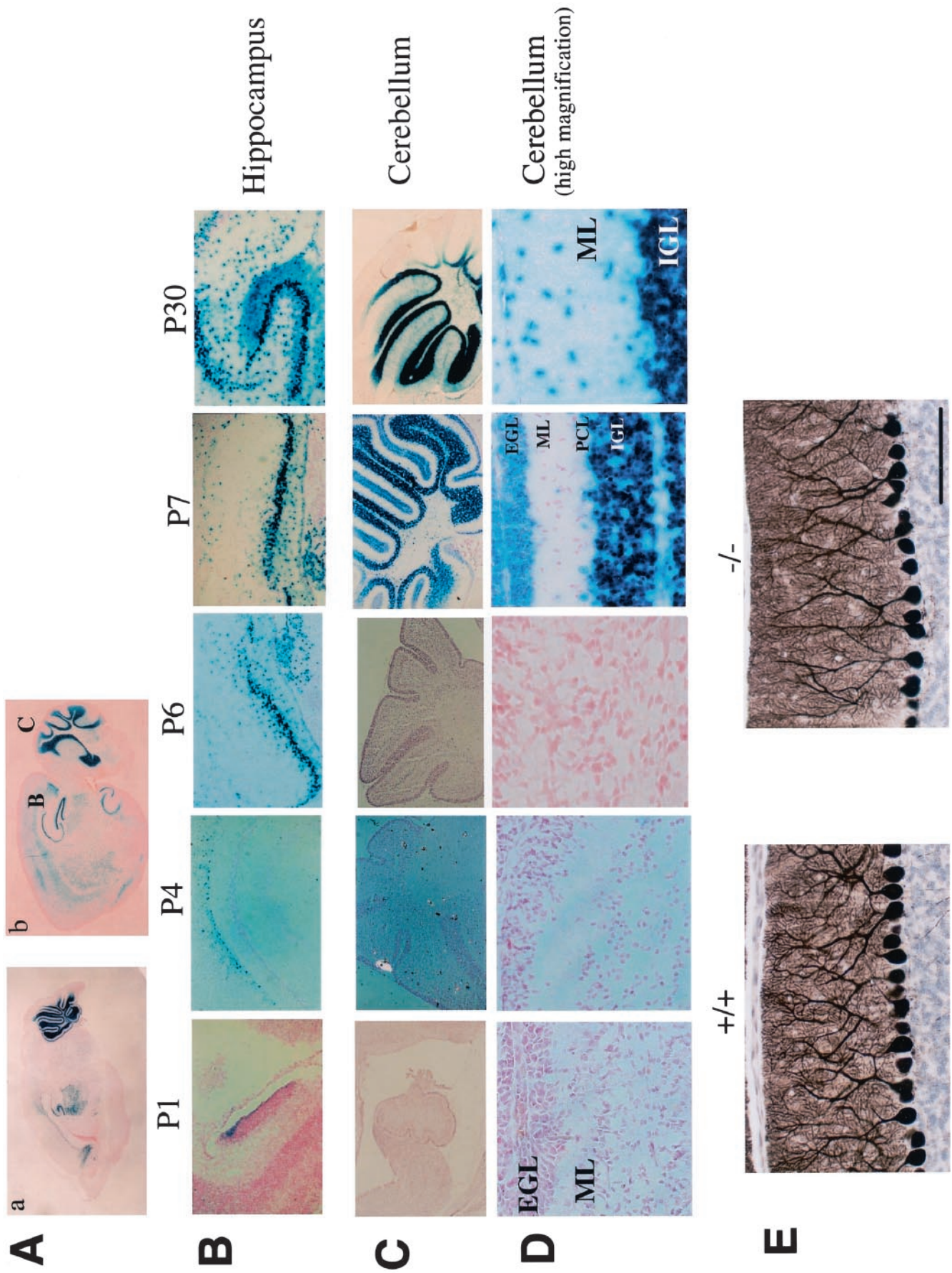
A
a   b   B   C

B   Hippocampus

C   Cerebellum

D   Cerebellum (high magnification)

P1   P4   P6   P7   P30

ML   IGL

EGL   ML   PCL   IGL

EGL   ML

E   +/+   -/-

FIG. 3. Spatiotemporal expression pattern of BTEB in the developmental process of mouse brain. β-Gal staining was performed with the brain of BTEB$^{+/-}$ heterozygous mice from stage P1 to P30. (A) Sagittal sections of brain from BTEB$^{+/-}$ heterozygous mutant mice at P7 (a) and P30 (b). The "B" and "C" labels in subpanel b indicate the areas of BTEB expression investigated in 3B (hippocampus) and 3C (cerebellum), respectively. (B) Temporal expression of BTEB in hippocampus at various postnatal stages. Heterozygous BTEB$^{+/-}$ mice were killed at P1, P4, P6, P7, and P30. Brains were removed and fixed for β-Gal staining. The brain specimens were cut at 10 μm. (C) Temporal expression pattern of BTEB in mouse cerebellum at various postnatal stages. The mouse brains were treated as described in panel B. BTEB expression was not detected during early postnatal stages but was detected distinctly at P7. (D) Magnified views of a part of cerebellar specimens in panel C. At P7, BTEB expression started in the external granular layer (EGL), the Purkinje cell layer (PCL), and internal granular layer (IGL). By P30, migration of external-granular-layer cells to the internal granular layer was complete. BTEB expression in the internal granular layer was preserved at P30, whereas its expression faded in the Purkinje cell layer and molecular layer. (E) Cerebellum sections of wild-type mice and homozygous BTEB mutant mice were stained with anti-IP$_3$R1 antibody to analyze the structure of Purkinje cells. Stained areas show dendritic shafts and spines of Purkinje cells.

idet P-40. For detection of β-Gal, specimens were soaked in PBS containing 20% sucrose, embedded in Tissue-Tek OCT compound (Sakura, Tokyo, Japan), and frozen in liquid nitrogen. Specimen sections of 30 μm were cut in a cryostat.

The TUNEL method was performed to detect apoptosis in brains according to the manufacturer's instruction (TaKaRa). Brains (P7) were fixed in neutralized formalin. Paraffin sections (3 μm) were subjected to the TUNEL experiment by using the in situ apoptosis detection kit (TAKARA).

Immunohistochemistry. Development of Purkinje cells was studied by immunostaining with an anti-IP$_3$R1 (1,4,5-inositol trisphosphate receptor 1) antibody. Dissected brains were fixed in Boun's solution for 2 h. Paraffin sections (8 μm thick) in the parasagittal plane were processed sequentially as described previously (27).

RNA analysis. mRNAs were analyzed by the reverse transcription-PCR (RT-PCR) method as described previously (28). Total RNA was prepared from mouse brains and aliquots (1 μg/ml) were reverse transcribed with random primers at 37°C for 60 min. The reverse transcripts were quantified by the PCR method. An aliquot (1 μl) of synthesized cDNA was amplified in a total volume of 20 μl containing 150 mM deoxynucleoside triphosphates, 0.2 U of *Taq* polymerase, and 0.12 μg of each pair of primers described below and [α-^{32}P]dCTP (4 μCi/20 μl). For BTEB, the 5′ and 3′ primers were 5′-ATG TCC GCG GCC GCC GCC GCC TAC AT-3′ and 5′-TCT GCA CTG TGG GAG GCC AG-3′, respectively. For β-actin control, the 5′ and 3′ primers were 5′-ATG GAT GAC GAT ATC GCT-3′ and 5′-ATG AGG TAG TCT GTC AGG 4T-3′, respectively. PCR was performed as 30 cycles of 30 s at 94°C, 30 s at 60°C, and 1 min at 72°C. The PCR products were analyzed on a 1% agarose gel with β-actin as a control.

Treatment of mice. In all experiments, littermates from cross-mating between BTEB$^{+/-}$ mice were used, and their genotypes were determined by PCR analysis of tail DNA samples. All of the mice used for the experiments were 10- to 15-week-old males. The mice were kept on a 12-h light-dark cycle at a constant temperature (23 ± 1°C). The tests were always conducted between 13:00 and 18:00. A week prior to the behavioral tests, one mouse was housed per cage and handled three times daily.

General activity. Locomotion and rearing behavior were measured by the method described previously (12) in an open-field box (32 by 32 by 20 cm) placed in a sound-attenuated room that was different from the room used for fear conditioning. Two pairs of a 7-by-7 array infrared photosensors were set against the outer wall and equally spaced in the lower and upper rows at intervals of 2 and 4.5 cm, respectively, above the floor. The frequency at which a photobeam was interrupted represented the movement of the animal and was recorded by computer. Each mouse was kept in the box for 30 min.

Light-dark choice test. The apparatus consisted of two compartments and was placed in a dark and sound-attenuated room. One compartment was a bright (250 lx) chamber of 16 by 32 by 20 cm illuminated by a white bulb (60 W), and the other was a dark (1 lx) chamber of the same dimensions. The two compartments were separated by a wall and connected by seven small openings (3 by 9 cm) through which the photobeam sensors passed. A mouse was placed in the center of the light chamber and its behavior was monitored by video camera. The mouse was considered to have entered the new area when all four feet were placed in that area. The following behavioral measures were scored: the time spent in the light and dark compartments, the number of transitions made between the two compartments, and the latency of the initial movement from the light to the dark room.

Rotorod test. The rotorod test was carried out as described previously (6). Mice were placed on a rod and the rod began to rotate at a constant velocity of 15 rpm. The test was continued for 3 min. The time that the mouse stayed on the rotating rod was measured. The test was done once a day for each mouse and repeated for 5 days.

Contextual fear conditioning. The experiment of contextual fear conditioning was performed as described previously (13). The conditioning chamber was an observation box (20 by 20 by 20 cm) constructed from clear and gray vinylchloride plates. The floor of the chamber consisted of 26 stainless steel rods through which foot shocks were delivered by means of a shock scrambler (SGS 002; Muromachi, Tokyo, Japan). The chamber was placed in a light and sound-attenuated room. A video camera placed in front of the chamber allowed the behavior of each mouse to be observed and recorded in an adjacent room. The shock scrambler and controller for conditioning was operated by remote in the same room. On the training day, each mouse was placed in the chamber for 2.5 min before it received three foot shocks (0.5 mA for 1 s with 2-min intervals). The mice were removed from the chamber 1 min after the last foot shock and returned to their original cages. At 24 h after training, the mice were returned to the chamber, and their behavior over a period of 6 min was observed in the absence of foot shocks. The extent of conditioned fear was measured by scoring the freezing behavior of the mice. Freezing was defined as the absence of visible
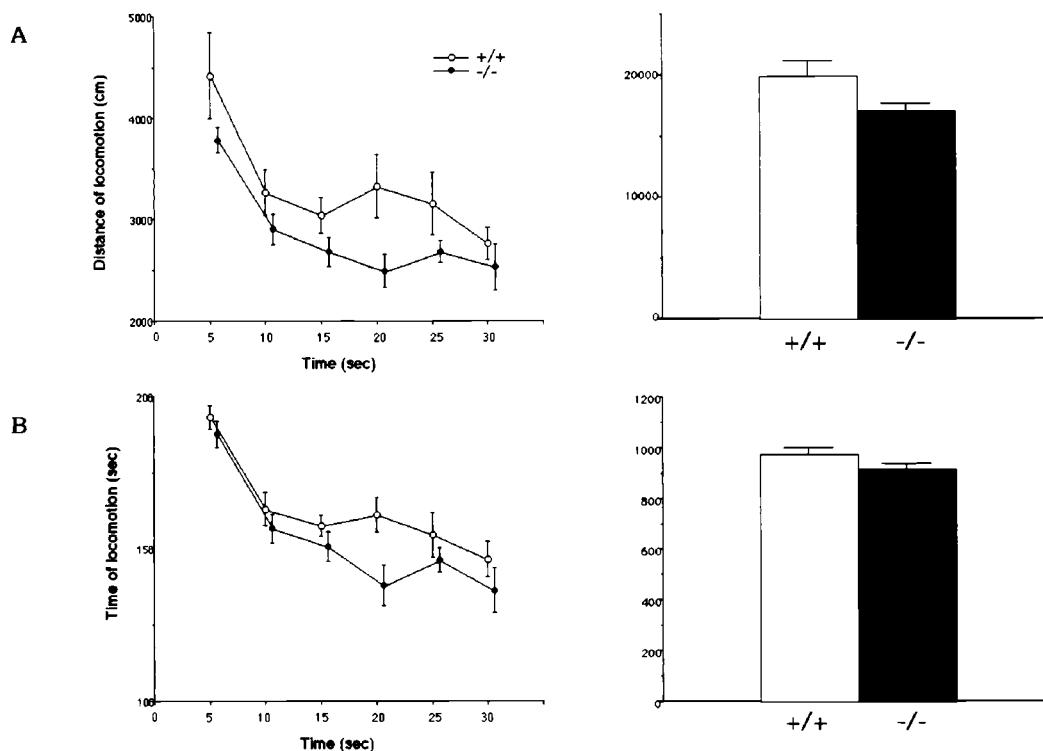
FIG. 4. Locomotion behaviors of BTEB$^{-/-}$ homozygous mutant and wild-type mice. Distance traveled during locomotion (A), time spent for horizontal movement (movement of more than 1 cm/s was counted) (B), frequency of rearing behavior (counts) (C), speed of movement (D), and the time spent in the light and dark compartments (E) for the preceding 5 min were measured and plotted for the total 30 min in the open-field test. Two pairs of array infrared photosensors were attached to the outer wall equally spaced in lower and upper rows, respectively, 2 and 4.5 cm above the floor. The lower row of photocells was used to measure locomotor activities, and the upper row was used to detect rearing behavior. A computer recorded the number of horizontal photobeam interruptions caused by animal movement. Each mouse was placed in the apparatus and left for 30 min, which was approximately the same time as when it received training trials in the afternoon. The points in the left panels show the average values of the locomotor activities for each 5 min in 30 min, and the bar graphs (right) show the average values of the total activities for 30 min with minimum deviation. In each experiment, wild-type mice ($n = 9$) and homozygous mutant mice ($n = 11$) were used.

movement, except for respiration. During the test period, two observers who were blind to the experimental conditions scored the tendency of the mice to freeze by watching the TV monitor. Observations were carried out by using a time-sampling procedure. For every 5 s during the test, the movement of each mouse was judged as either frozen or active. An unbiased estimate of the actual time spent in the frozen position was calculated per minute. After completion of the first fear conditioning test, the mice were returned to their original cages for 24 h and then subjected to a second contextual fear test carried out in the same way as the first.

Electric shock sensitivity test. Since the sensitivity to foot shocks may affect freezing responses, we measured the minimal level of current required for mice to elicit vocalization and jumping by the method described previously (12) after general activity and light-dark choice tests.

Each mouse was placed in the chamber used for the contextual fear conditioning and delivered 1-s shocks of increasing intensity. The interval between shocks was 10 s. The sequence of current used was as follows: 0.05, 0.08, 0.1, 0.2, 0.3, 0.4, 0.5, 0.6, and then 0.8 mA. The minimal level of current required to elicit vocalization and jumping was determined. These experiments were performed in a blind manner.

Other activity tests. The horizontal wire-hanging, rod-walking, and gait tests were performed as described previously (13).

Data analysis. Data were analyzed by one- or two-way analysis of variance, and comparison of the paired groups was carried out by the Fisher latest significant difference test. All values in the text and figure legends are expressed as mean values $\pm$ the standard errors of the mean, where n is the number of mice tested.

RESULTS

Targeted disruption of the BTEB gene. Part of the 129/SV mouse BTEB genomic fragment of the targeting vector was replaced by *lacZ* positioned in frame with the BTEB gene. By this means, β-Gal expression mimics the mode of BTEB expression in the homologous recombinant mice and, therefore, facilitates assessment of pathological defects owing to a disrupted BTEB gene (Fig. 1A). The linearized plasmid was introduced into E14 ES cells by electroporation, and the cells were subjected to double selection by using G418 and ganciclovir. PCR analysis and subsequent DNA blot analysis of the DNAs extracted from the resistant clones revealed that, of 268 clones screened, 10 represented legitimate homologous recombination (Fig. 1B). Mutant ES cells were proliferated and microinjected into C57BL/6j blastocysts to give rise to chimeric animals, as judged from coat color. Male chimeras were mated with C57BL/6j females to give heterozygotes possessing the BTEB gene, which were then interbred to yield homozygous BTEB$^{-/-}$ mutant mice. DNA blot analysis with genomic tail DNAs from 103 offspring born from heterozygous matings revealed that the ratio of wild-type BTEB$^{+/+}$ to heterozygous BTEB$^{+/-}$ to homozygous BTEB$^{-/-}$ mice was 27:54:22, which represents the 1:2:1 ratio expected from the normal Mendelian rule (Fig. 1C and D). Homozygous mutant BTEB$^{-/-}$ mice appeared to grow normally and were fertile without any evident pathological defects, indicating that the BTEB gene is not essential for survival or fertility. BTEB mRNA levels were not
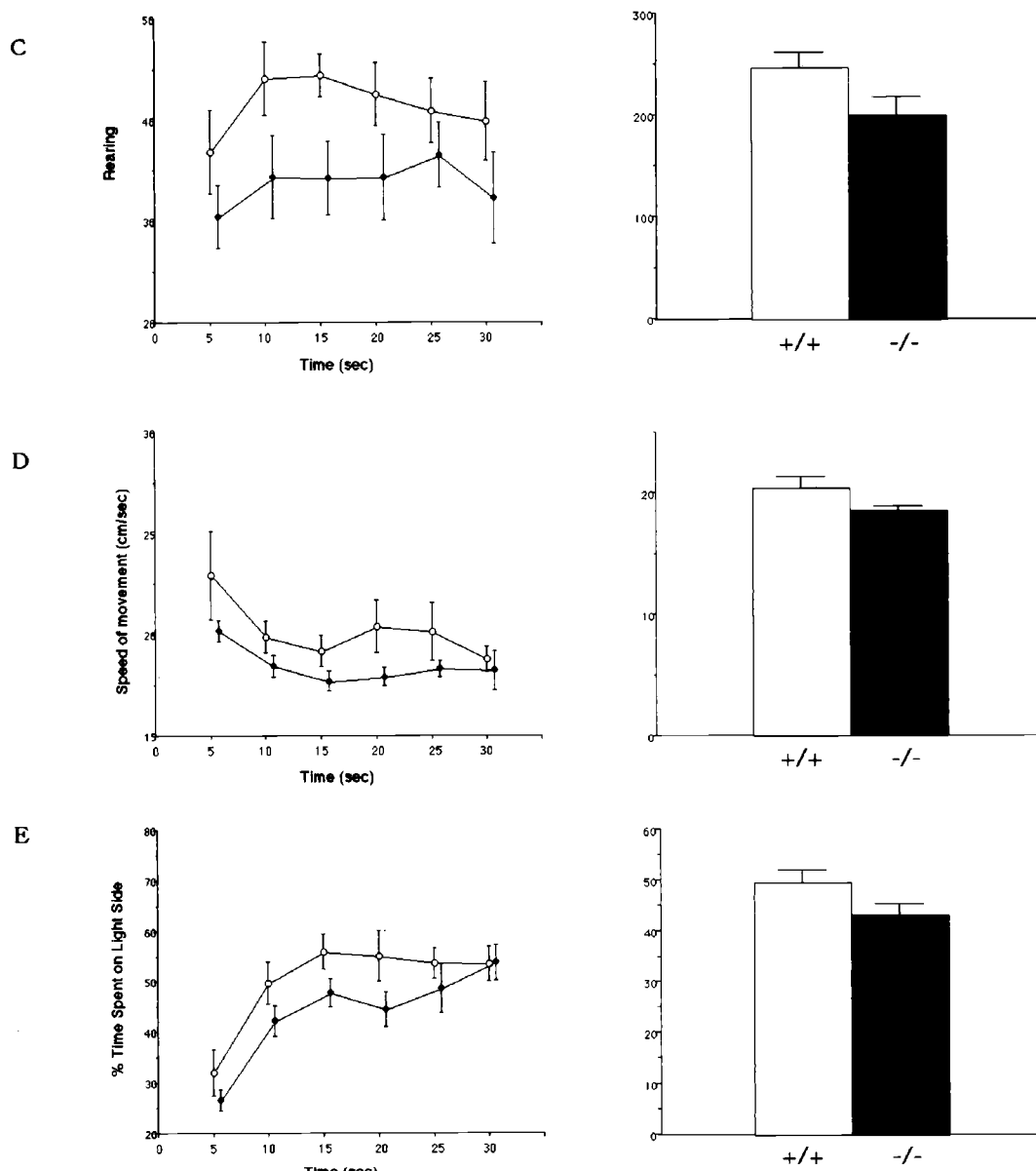
FIG. 4—*Continued.*

detected by RT-PCR analysis with RNA isolated from the brains of adult mutant BTEB$^{-/-}$ mice, indicating perfect disruption of the BTEB gene (Fig. 1E).

Expression of BTEB as revealed by in situ hybridization and β-Gal staining. To investigate the expression pattern of BTEB, we compared β-Gal staining with immunoblot analysis of BTEB with an anti-BTEB antibody at various embryonic stages. The pattern of immunostaining of BTEB generally concurred with that of β-Gal staining (Fig. 2D). Hence, we investigated the expression of BTEB by β-Gal staining. Expression of β-Gal in BTEB$^{+/-}$ mice was essentially the same as that in BTEB$^{-/-}$ mice, indicating that homozygous deletion of the BTEB gene does not result in gross alterations in the formation and development of various organs and tissues. The β-Gal

staining revealed that BTEB expression commenced in skeletal structures at E12.5 and spread ubiquitously throughout various tissues except lung (Fig. 2Aa, Ab, and C). In particular, BTEB showed a very characteristic and potent regional expression in the brain (Fig. 3A). BTEB expression was detected in the hippocampus from P1 and was distinctive in the pyramidal cell layer at P6, and significant expression occurred in the cortical layer of the cerebellum at P7, whereas its expression was rather limited in Purkinje cells (Fig. 3B, C, and D). Taken together with the report that forced expression of BTEB by DNA transfection experiments induced the outgrowth of dendrites in Neuro-2A cells, the dynamic expression of BTEB in the developing mouse brain led us to consider that BTEB might be important in the formation of the cerebellum. We compared
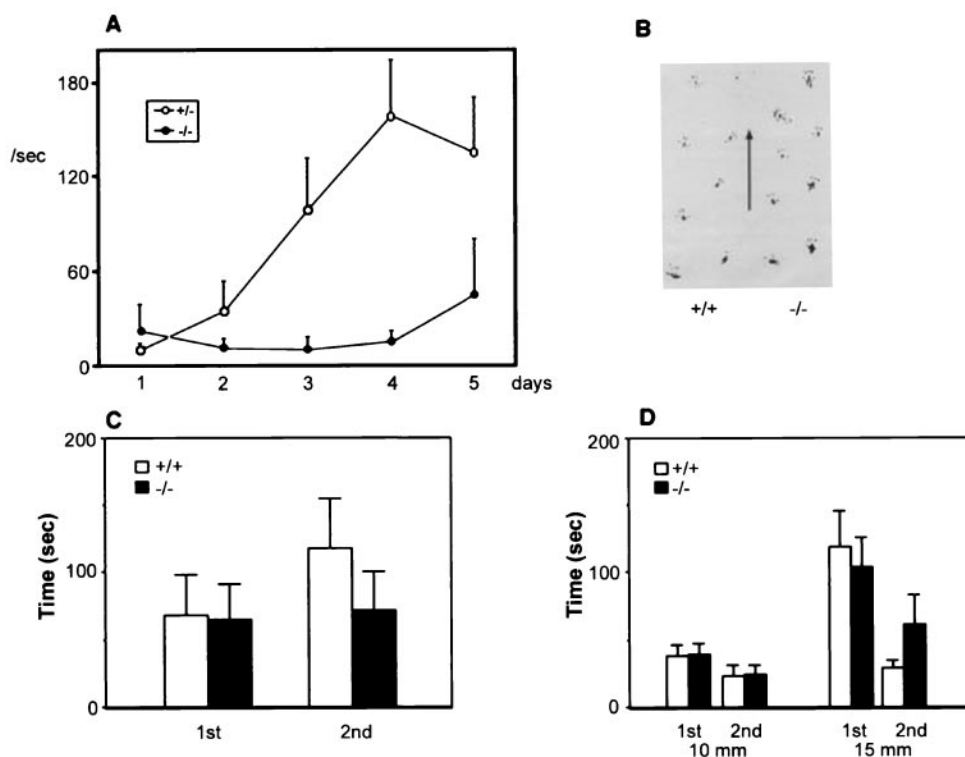
FIG. 5. Rotorod performance in BTEB$^{-/-}$ mutant and wild-type mice. (A) Rotorod test. Fall latencies of the mutant BTEB$^{-/-}$ and wild-type mice on a rod rotating at 15 rpm was measured for 1 s once a day for a consecutive 5 days. Wild-type ($n = 9$) and mutant mice ($n = 11$) were used. A maximum of 180 s was tested for each animal per trial. (B) Gait measurement. Representative foot spots of heterozygous and homozygous mutant mice are presented. (C) Horizontal wire-hanging test. Mice were hung on the elevated horizontal wire by the forepaws, and the time in seconds of their hanging on the wire was measured until they fell off the wire. (D) Rod-walking test. Mice were placed on the midpoint of the wooden rod (10 or 15 mm diameter, 60 cm in length), and the time in seconds required for the mice to cross the rod wire was measured. At least nine animals were tested for each genotype.

the morphology of the BTEB$^{-/-}$ cerebellum with that of the wild type by using anti-IP$_3$R1 antibody. Although no marked difference was found between the BTEB-null and the wild-type mice (Fig. 3E), there appeared to be a slightly poorer development of Purkinje cell dendrites in the BTEB-null mice. We performed the TUNEL assay of the cerebellum specimens of the wild-type and the homozygous mutant mice at P7 to see whether apoptosis may occur in this tissue of the mutant mice. However, no noticeable apoptosis signal was found in this tissue of either mutant or wild-type mice at P7 (data not shown). Dendrite development of Purkinje cells in the BTEB-null mice needs to be investigated in a more quantitative manner.

Behavioral assessment of BTEB$^{-/-}$ mutants. From the expression mode of BTEB during mouse brain development and from the transcriptional function of BTEB as a target of T$_3$, we postulated the involvement of BTEB in learning and memory tasks associated with hippocampal function and in motor coordination related to cerebellar function. We performed systematic analysis of the gross neurogenic and motor functions in BTEB$^{-/-}$ mice.

(i) General activity. We measured, as the basis of the behavioral tests, general activities such as locomotion (distance and time), rearing, speed of movement, and choice between light and dark (Fig. 4). The mean activity counts of locomotion

and rearing behaviors for 30 min are shown in Fig. 4. These activities of locomotion and rearing behavior appeared to be slightly lower in homozygous mutant BTEB$^{-/-}$ mice than in wild-type mice (19,988.4 $\pm$ 77.8 cm and 248.8 $\pm$ 21.5 for the wild type and 17,086.5 $\pm$ 74.5 cm and 202.3 $\pm$ 22.4 for the mutant mice, respectively). However, analysis of variance indicated insignificant differences in the locomotor activity [$F(1,108) = 14.66, P < 0.001$] and rearing behavior [$F(1,108) = 14.89, P < 0.001$] between wild-type and BTEB$^{-/-}$ mice, so we did not expect this mild impairment in general activities to greatly influence other behavioral tests (Fig. 4)

Any difference in the internal emotion between wild-type and BTEB$^{-/-}$ mice might affect their performance in the contextual fear conditioning test. Therefore, we carried out a light-dark choice test (Fig. 4E), considered to be a measure of anxiety or fear-related emotion in rodents. The mean percent time spent in the light side was as follows: 50% $\pm$ 2% for wild-type mice and 44% $\pm$ 2% for BTEB$^{-/-}$ mice. These data were not considered to be significantly different between wild-type and BTEB$^{-/-}$ mice, suggesting that BTEB$^{-/-}$ mice do not have a severe emotional disorder related to anxiety and fear.

(ii) Rotorod test. Since BTEB was clearly demonstrated to be expressed in Purkinje cell layers of the cerebellum (Fig. 3), we carried out the rotorod task, which is associated with cer-
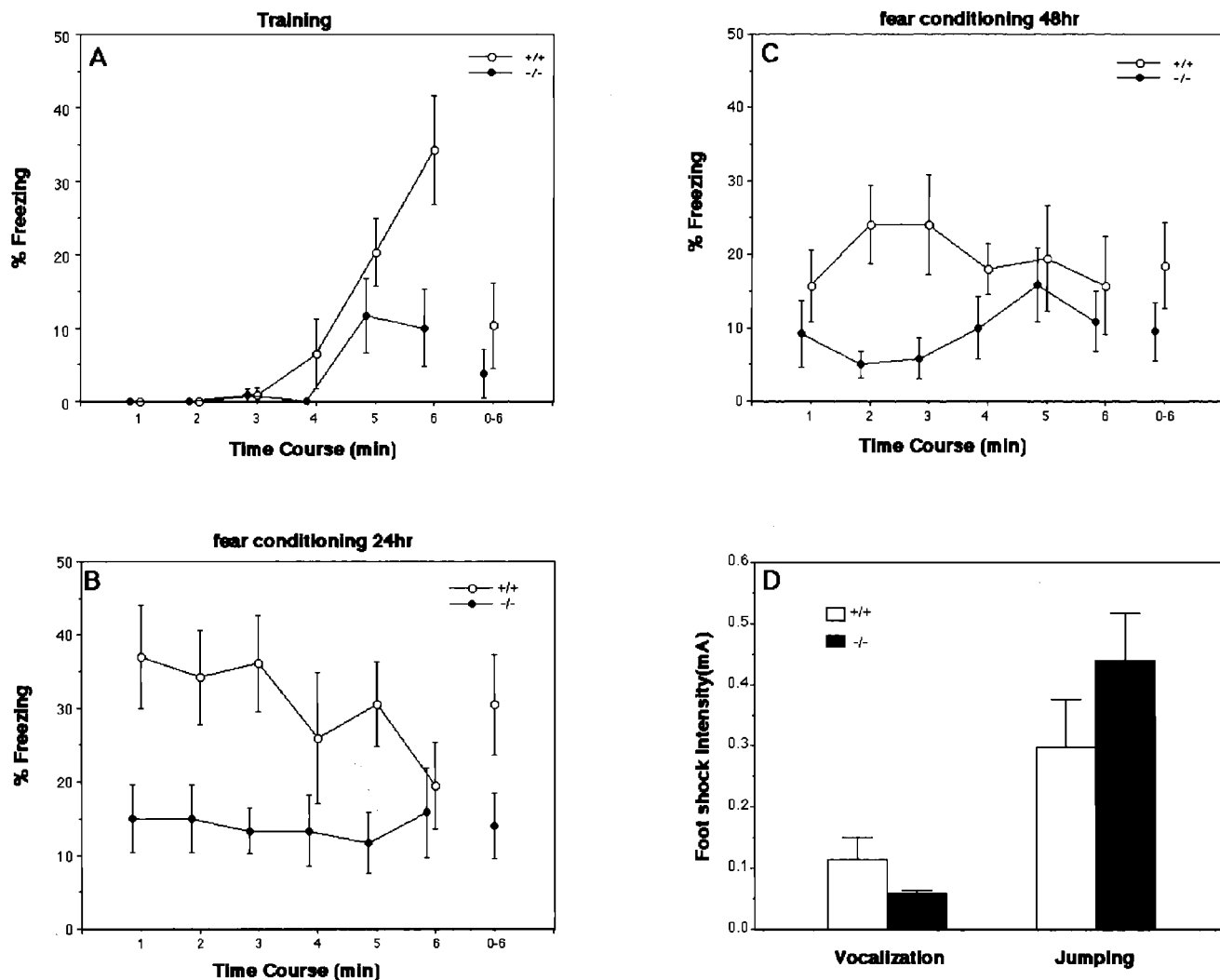
FIG. 6. Contextual fear conditioning task of the wild-type and homozygous BTEB$^{-/-}$ mutant mice. (A) Mean percentages of freezing before and during three foot shocks were determined at 5-s intervals. Three 1-s foot shocks (0.5 mA) were given 3, 4, and 5 min after animals had been placed in a new foot shock-equipped chamber. (B) Mean percentages of freezing behavior of the animals 24 h after the footshock. The foot shock-treated animals in panel A were returned to their original cages for 24 h. Immediately the animals were returned to the footshock chamber, the percentages of freezing behavior of the mice were counted. (C) After the experiments in panel B, the mice were returned to their original cage for another 24 h and then subjected to the same task as in panel B. Observations were carried out by using a time-sampling procedure. For every 5 s, each mouse was judged as either freezing or active during the test. The values were expressed as the average percentages of the mice used for each group with minimal deviations. (D) Sensitivity to foot shock. Sensitivity to foot shock was quantified by measuring minimal levels of current required to elicit two stereotypical behaviors: vocalization and jumping. In each experiment, wild-type mice ($n = 9$) and homozygous mice ($n = 11$) were used.

ebellar function (Fig. 5A). In addition to the general activities described, gait behavior (Fig. 5B), horizontal wire hanging (Fig. 5C), and rod walking (Fig. 5D) were examined as the basis of the rotorod test. In these tests, homozygous BTEB$^{-/-}$ mutant and wild-type mice did not show so much difference as to physically affect the rotorod test. In this task, animals must make continuous adjustments to their balance and posture in order to keep upright on a rod rotating at a constant velocity during each 5-min trial. In general, the BTEB$^{-/-}$ mice ($n = 9$) exhibited a significant performance deficit compared with the heterozygous BTEB$^{+/-}$ mutant mice ($n = 14$) (Fig. 5A). On the first day of the experiment, no mouse could stay on the rotating rod for a long time, regardless of the genotype. How-

ever, while days of training clearly improved the adjustment performance of heterozygous mice, BTEB$^{-/-}$ mice did not show improved performance in the rotorod test after daily training. These data suggest that the basis of the performance deficit of BTEB$^{-/-}$ mice on the rotorod test is in motor learning and motor coordination (Fig. 5A).

(iii) Contextual fear conditioning. BTEB is also distinctly expressed in the hippocampus and amygdala (Fig. 3). Since contextual fear conditioning requires correct functioning of both the hippocampus and amygdala, we tested BTEB$^{-/-}$ mice in context-dependent fear conditioning (Fig. 6). Fear conditioning is based on the ability of normal animals to fear a previous neural stimulus, or conditioned stimulus, because of

its temporal association with an adverse stimulus such as a foot shock. When reexposed to the conditioned stimulus, conditioned animals tend to refrain from all but respiratory movement, a response known as freezing. The percentage of time spent in freezing was quantified. During the conditioning phase of the experiment, mice were placed in the shock chamber and received three 1-s foot shocks at 1-min intervals. In the early phase of the experiment, before the first foot shock, a baseline activity was assessed for the BTEB$^{-/-}$ mutant and wild-type mice. Baseline fear during the first 3 min was characteristically low and did not differ across genotype (Fig. 6A). When foot shocks were given to the mice, both wild-type and BTEB$^{-/-}$ mutant groups showed significantly increased freezing behavior during training, although BTEB$^{-/-}$ mice appeared to be slightly more defective in their freezing response compared to the wild type (Fig. 6A). After the three foot shocks, the experimental animals were returned to their original cages. After 20 h, mice were placed in the same conditioning chamber and monitored for freezing behavior, which was characterized by an immobile and crouching posture. Both BTEB$^{-/-}$ mutant and wild-type mice displayed the conditioned freezing response in the training context. However, mutants froze significantly less than did the wild-type mice, indicating a moderate deficit in context-dependent fear conditioning (Fig. 6B). The mice under examination were again returned to their original cages. After an additional 24 h, the mice were again subjected to the test of contextual fear conditioning. Although mice with a wild-type BTEB genotype again displayed the conditioned freezing response, albeit to a lesser extent than the previous trial, the BTEB$^{-/-}$ mutant mice still showed a significant deficit in contextual freezing response relative to the wild-type mice (Fig. 6C). We then tested whether or not BTEB$^{-/-}$ mice have an altered nociceptive reaction to shock, because changes in pain sensitivity can affect performance on the fear conditioning test. For both BTEB$^{-/-}$ and wild-type mice, we determined the threshold current for eliciting two progressive reactions, jumping and vocalization, in response to increasing electrical foot shocks (Fig. 6D). The results of these experiments showed that there was little difference, if any, in the jumping and vocalization reaction between the BTEB$^{-/-}$ mutant and wild-type mice. The level of current required to induce vocal responses from the BTEB$^{-/-}$ mice (0.058 ± 0.006 mA) was a little lower than that for the wild-type mice [0.114 ± 0.036 mA; $F(1,17) = 1.72$, $P = 0.207$], whereas the reverse was observed in the jumping behavior [0.30 ± 0.08 mA for wild-type mice and 0.44 ± 0.08 mA for BTEB$^{-/-}$ mutants; $F(1,17) = 1.72$, $P = 0.207$]. These data indicated that the pain sensitivity and physical response to pain were not so different between the wild-type and BTEB$^{-/-}$ mutant mice and thus were not considered to affect performance in fear conditioning.

DISCUSSION

BTEB belongs to the Sp1/XKLF family of transcription factors with characteristic triple repeat C2H2 zinc finger motifs (15). Despite their similarity in primary structure and DNA-binding property, these factors have unique functions. It has been demonstrated from gene targeting experiments that Sp1-, Sp3-, and Sp4-deficient mice display very different phenotypes.

Retarded development was observed in Sp1$^{-/-}$ mutant embryos, and they showed a broad range of abnormalities, resulting in embryonic death around day 11 of gestation. The expression of many putative target genes, including cell cycle-regulated genes, was not significantly affected in Sp1$^{-/-}$ embryos, except for reduced MeCP2 expression (22). On the other hand, Sp3 deficiency resulted in embryonic growth retardation and neonatal death because of respiratory failure, the cause of which remains obscure (2). Histological examinations of various organs of the Sp3$^{-/-}$ mutant mice revealed a pronounced defect in late tooth formation due to an impaired dentin or enamel layer of the developing teeth. In Sp4$^{-/-}$ mutant mice, postnatal death occurred in two of the neonates within the first few days. The remaining Sp4$^{-/-}$ mutants showed retarded growth compared to wild-type littermates, and males were defective in reproduction (31). Compared to Sp1, BTEB is a smaller protein consisting of 244 amino acids with a high sequence similarity to Sp1 in the zinc finger domain and has a closely similar binding affinity toward the GC-box sequence (15). As described previously, however, unique properties of translational regulation and T$_3$-inducible expression of BTEB prompted us to produce BTEB-defective mice to aid understanding of the physiological roles of BTEB and, at least, a part of the function of thyroid hormone T$_3$. Matings between heterozygous BTEB$^{+/-}$ mutant mice gave female and male BTEB$^{-/-}$ pups according to normal Mendelian genetics, and these animals grew apparently normally and were fertile. BTEB expression was first observed in the tip of the nasal bone at E12.5, and expression continued to spread throughout various tissues and organs up until parturition. Generally speaking, BTEB was expressed ubiquitously in adult animals and displayed characteristically potent expression in the hippocampus, cerebellum, and bone. By comparing β-Gal staining between BTEB$^{-/-}$ and BTEB$^{+/-}$ mice, we investigated whether BTEB deficiency caused any abnormality in organogenesis, paying special attention to the skeleton, hippocampus, and cerebellum. However, we could not find any gross morphological alterations in these tissues of BTEB$^{+/-}$ and BTEB$^{-/-}$ mice. Immunostaining with anti-IP$_3$R1 antibody showed that dendrites sprouting from Purkinje cells appeared to be slightly decreased in BTEB$^{-/-}$ mice. Although this seems to be consistent with the enhanced neurite outgrowth seen with overexpression of BTEB in Neuro-2A cells (4), precise quantitative analysis of the dendrite formation needs to be carried out by other methods such as electron microscopy. These results imply that BTEB is not involved in the gross morphogenesis of these organs at the light microscopic level or that other members of the Sp family may be compensating for the BTEB$^{-/-}$ deficiency.

On the other hand, we found that mouse behavior was significantly affected by BTEB deficiency. Detailed and systematic analyses in gross neurological and motor tasks of the BTEB$^{-/-}$ mutants revealed only slight differences in locomotor activities, rearing behavior, and speed of movement or no difference in the rod-walking test, light-dark choice test, horizontal wire-hanging test, or gait measurements compared to wild-type mice. However, we observed a performance deficit in BTEB$^{-/-}$ mice on the rotating rod, a test considered to involve the function of the cerebellum. Although sensorimotor learning and, therefore, performance on the rotarod cannot easily

be attributed to a single brain region, it is widely accepted that the cerebellum is a major component involved in this task (19). Mice with structural abnormalities in the cerebellum or with disruptions in genes richly expressed in the cerebellum exhibit performance deficits on the rotorod (17, 30). The performance deficit of BTEB$^{-/-}$ mice in the rotorod test is consistent with the defective function of BTEB that showed enhanced expression in the cerebellum. In the cerebellum, dynamic BTEB expression was initiated at P7, around the time when synapse formation starts to mature in the mouse brain (8). The formation of the synapses in BTEB$^{-/-}$ mice should be quantitatively analyzed in more detail to see whether the defective rotorod performance of BTEB$^{-/-}$ mice is due to impaired synapse formation.

In connection with the marked expression of BTEB in the pyramidal cell layers of the hippocampus, the BTEB$^{-/-}$ mice displayed a marked defect in contextual freezing response. The freezing deficit of the mutant mice was observed both immediately (immediate after shock freezing) and 1 day (delayed freezing) after the shock was presented. Since several control experiments indicated that BTEB deficiency caused neither a sensory nor a motor performance deficit in the response to foot shock, this result implies that BTEB$^{-/-}$ mice have deficits in the acquisition and preservation of memory. Although various brain areas are considered to be implicated in the process of contextual fear conditioning, the neural circuits of the hippocampus and amygdala, in particular, are responsible for contextual fear conditioning (1, 7, 16, 25). Since BTEB expression increased in the pyramidal cells of the hippocampus at P7 when synapses began to mature in the brain, it is possible that the impaired fear response in the BTEB-deficient mice resulted from impaired synapse formation in the hippocampus. The possible involvement of BTEB in synapse formation is supported by the enhanced neurite outgrowth of Neuro-2A cells resulting from the overexpression of BTEB (4). Additional experiments, such as the water maze test (23) and the conditioning taste aversion test (21, 36), are necessary to determine whether BTEB deficiency causes defective neural processes that are dependent on the hippocampus, the amygdala, or both. It would also be worthwhile and interesting to investigate the target genes of BTEB for further understanding the function of BTEB itself and, at least, a part of T$_3$ function in the development of the central nervous system. The distinct behavioral abnormalities of the BTEB knockout mice and characteristic expression pattern of BTEB will provide a useful system for further investigation of the mechanisms underlying motor function, learning, and memory.

ACKNOWLEDGMENTS

REFERENCES

1. **Anagnostares, S. G., S. Maron, and M. S. Fenselow.** 1999. Temporally graded retrograde amnesia of contextual fear after hippocampal damages in rats: within-subject exmination. J. Neurosci. **19:**1106–1114.
2. **Bouwman, P., H. Gollner, H. P. Elsasser, G. Eckhoff, A. Karis, F. Grosveld, S. Philipsen, and G. Suske.** 2000. Transcription factor Sp3 is essential for post-natal survival and late tooth development. EMBO J. **19:**655–661.
3. **Brown, D. D., Z. Wang, J. D. Furlow, A. Kanamori, R. A. Schwartzman, B. F. Remo, and A. Pinder.** 1996. The thyroid hormone-induced tail resorption program during *Xenopus laevis* metamorphosis. Proc. Natl. Acad. Sci. USA **93:**1924–1929.
4. **Denver, R. J., L. Ouellet, D. Furling, A. Kobayashi, Y. Fujii-Kuriyama, and J. Puymirat.** 1999. Basic transcription element-binding protein (BTEB) is a thyroid hormone-regulated gene in the developing central nervous system: evidence for a role in neurite outgrowth. J. Biol. Chem. **274:**23128–23134.
5. **Denver, R. J., S. Pavgi, and Y. B. Shi.** 1997. Thyroid hormone-dependent gene expression program for *Xenopus* neural development. J. Biol. Chem. **272:**8179–8188.
6. **Ferguson, G. D., S. G. Anagnostaras, A. J. Silva, and H. R. Herschman.** 2000. Deficit in memory and motor performance in synaptotagmin IV mutant mice. Proc. Natl. Acad. Sci. USA **97:**5598–5603.
7. **Frankland, P. W., V. Cestari, R. K. Filipkowski, R. J. McDonald, and A. J. Silva.** 1998. The dorsal hippocampus is essential for context discrimination but not for contextual conditioning. Behav. Neurosci. **112:**863–874.
8. **Gaarskjaer, F. B.** 1985. The development of the dentate area and the hippocampal mossy fiber projection of the rat. J. Comp. Neurol. **24:**1154–1170.
9. **Hogan, B., R. Beddington, F. Constantini, and E. Lacy.** 1994. Manipulating the mouse embryo: a laboratory manual, p. 277–290. Cold Spring Harbor Laboratory, Cold Spring Harbor, N.Y.
10. **Iglesias, T., A. Caubin, G. H. Stunnenberg, A. Zaballos, J. Bernal, and A. Minoz.** 1996. Thyroid hormone-dependent transcriptional repression of neural adhesion molecule during brain maturation. EMBO J. **15:**4307–4316.
11. **Iglesias, T., A. Caubin, J. Zaballos, J. Berna, and A. Munoz.** 1995. Identification of mitochondrial NADH dehydrogenes submit 3(ND3) as a thyroid hormone regulated gene by whole genome PCR analysis. Biochem. Biophys. Res. Commun. **210:**995–1100.
12. **Ikegami, S.** 1994. Behavioral impairment in radial-arm maze learning and acetylcholine content of the hippocampus and cerebral cortex in aged mice. Behav. Brain Res. **65:**103–111.
13. **Ikegami, S., A. Harada, and N. Hirokawa.** 2000. Muscle weakness, hyperactivity, and impairment in fear conditioning in tau-deficient mice. Neurosci. Lett. **279:**129–132.
14. **Imataka, H., K. Nakayama, K. Yasumoto, A. Mizuno, Y. Fujii-Kuriyama, and M. Hayami.** 1994. Cell-specific translational control of transcription factor BTEB expression. The role of an upstream AUG in the 5'-untranslated region. J. Biol. Chem. **269:**20668–20673.
15. **Imataka, H., K. Sogawa, K. Yasumoto, Y. Kikuchi, K. Sasano, A. Kobayashi, M. Hayami, and Y. Fujii-Kuriyama.** 1992. Two regulatory proteins that bind to the basic transcription element (BTE), a GC box sequence in the promoter region of the rat P-4501A1 gene. EMBO J. **36:**63–71.
16. **Kim, J. J., and M. S. Fanselow.** 1992. Modality-specific retrograde amnesia of fear. Science **256:**675–677.
17. **Lalonde, R., A. N. Bensoula, and M. Filali.** 1995. Rotorod sensorimotor learning in cerebellar mutant mice. Neurosci. Res. **42:**3–6.
18. **Legrand, J.** 1983. Thyroid hormones and maturation of the nervous system. J. Physiol. **78:**603–542.
19. **Llinas, R., and J. P. Welsh.** 1993. On the cerebellum and motor learning. Curr. Opin. Neurobiol. **9:**58–65.
20. **Mangelsdorf, D. J., C. Thummel, M. Beato, P. Herrlich, G. Schutz, K. Umesono, B. Blumberg, P. Kastner, M. Mark, P. Chambon, and R. M. Evans.** 1995. The nuclear receptor superfamily: the second decade. Cell **83:**835–839.
21. **Masugi, M., M. Yokoi, R. Shigemoto, K. Muguruma, Y. Watanabe, G. Sansig, H. Van der Putten, and S. Nakanishi.** 1999. Metabstrozic glutamate receptor subtype 7 ablation causes deficit in fear response and conditioned taste aversion. J. Neurosci. **19:**55–63.
22. **Marin, M., A. Karis, P. Visser, F. Grosveld, and S. Philipsen.** 1997. Transcription factor Sp1 is essential for early embryonic development but dispensable for cell growth and differentiation. Cell **89:**619–628.
23. **Morris, R. G., P. Garrud, J. N. Rawlins, and J. O'Keefe.** 1982. Place navigation impaired in rats with huppocampol lesions. Nature **297:**681–683.
24. **Munoz, A. A., A. Rodriguez-Pena, A. Perez-Castillo, B. Ferreiro, J. G. Sutcliffe, and J. Bernal.** 1991. Effect of neonatal hypothyroidism on rat brain gene expression. Mol. Endocrinol. **5:**273–280.
25. **Phillips, R. G., and J. E. LeDoux.** 1985. Differential contribution of amygdala

and hippocampus to cued and contextual fear conditioning. Behav. Neurosci. **106:**274–285.

26. **Porterfield, S. P., and C. E. Hendrich.** 1993. The role of thyroid hormones in prenatal and neonatal neurological development: current perspectives. Endocrinol. Rev. **14:**94–106.

27. **Ryo, Y., A. Miyawaki, T. Furuichi, and K. Mikoshiba.** 1993. Expression of the metabolic glutamate receptor mGluR1 alpha and the ionotropic glutamate receptor GluR1 in the brain during postnatal development of normal mouse and in the cerebellum from mutant mice. J. Neurosci. Res. **36:**19–32.

28. **Sambrook, J., E. F. Fritsch, and T. Maniatis.** 1989. Molecular cloning: a laboratory manual, 2nd ed. Cold Spring Harbor Laboratory Press, Cold Harbor, N.Y.

29. **Sogawa, K., Y. Kikuchi, H. Imataka, and Y. Fujii-Kuriyama.** 1993. Comparison of DNA-binding properties between BTEB and Sp1. J. Biochem. **114:**605–609.

30. **Storm, D. R., C. Hansel, B. Hacker, A. Parent, and D. J. Linden.** 1998. Impaired cerebellar long-term potentiation in type I adenylyl cyclase mutant mice. Neuron **1:**199–210.

31. **Supp, D. M., D. P. Witte, W. W. Branford, E. P. Smith, and S. S. Potter.** 1996. Sp4, a member of the Sp1-family of zinc finger transcription factors, is required for normal murine growth, viability, and male fertility. Dev. Biol. **176:**284–299.

32. **Thompson, C. C.** 1996. Thyroid hormone-responsive genes in developing cerebellum include a novel synotogamine and a hairless homolog. J. Neurosci. **16:**7832–7840.

33. **Tsai, M. J., and B. W. O'Malley.** 1994. Molecular mechanisms of action of steroid/thyroid receptor superfamily members. Annu. Rev. Biochem. **63:**451–486.

34. **Ussault, J. H., and J. Ruel.** 1987. Thyroid hormones and brain development. Annu. Rev. Physiol. **49:**321–334.

35. **Vega-Nunez, E., R. Menendez-Hurtado, A. Garesse, A. Santos, and A. Perez-Castillo.** 1995. Thyroid hormone-regulate brain mitochondrial genes revealed by differential cDNA cloning. J. Clin. Investig. **89:**3–9.

36. **Yamamoto, T., Y. Fujimoto, T. Shimura, and N. Sakai.** 1995. Conditioned taste aversion in rats with excitotoxic brain lesion. Neurosci. Res. **22:**31–49.